



Ultrafast non-thermal laser excitation of gigahertz longitudinal and shear acoustic waves in spin-crossover molecular crystals [Fe(PM-AzA)(2)(NCS)(2)]

T. Parpiiev, M. Servol, Maciej Lorenc, Ievgeniia F Chaban, R. Lefort, Eric Collet, H. Cailleau, P. Ruello, Nathalie Daro, Guillaume Chastanet, et al.

► To cite this version:

T. Parpiiev, M. Servol, Maciej Lorenc, Ievgeniia F Chaban, R. Lefort, et al.. Ultrafast non-thermal laser excitation of gigahertz longitudinal and shear acoustic waves in spin-crossover molecular crystals [Fe(PM-AzA)(2)(NCS)(2)]. Applied Physics Letters, 2017, 111 (17), 179901 (2 p.). 10.1063/1.5009657 . hal-01681154

HAL Id: hal-01681154


<https://univ-rennes.hal.science/hal-01681154>

Submitted on 23 Jan 2018

HAL is a multi-disciplinary open access archive for the deposit and dissemination of scientific research documents, whether they are published or not. The documents may come from teaching and research institutions in France or abroad, or from public or private research centers.

L'archive ouverte pluridisciplinaire **HAL**, est destinée au dépôt et à la diffusion de documents scientifiques de niveau recherche, publiés ou non, émanant des établissements d'enseignement et de recherche français ou étrangers, des laboratoires publics ou privés.

AUTHOR QUERY FORM

	Journal: Appl. Phys. Lett. Article Number: 032741APL	Please provide your responses and any corrections by annotating this PDF and uploading it according to the instructions provided in the proof notification email.
---	---	--

Dear Author,

Below are the queries associated with your article; please answer all of these queries before sending the proof back to AIP.

Article checklist: In order to ensure greater accuracy, please check the following and make all necessary corrections before returning your proof.

1. Is the title of your article accurate and spelled correctly?
2. Please check affiliations including spelling, completeness, and correct linking to authors.
3. Did you remember to include acknowledgment of funding, if required, and is it accurate?

Location in article	Query / Remark: click on the Q link to navigate to the appropriate spot in the proof. There, insert your comments as a PDF annotation.
AQ1	Please check that the author names are in the proper order and spelled correctly. Also, please ensure that each author's given and surnames have been correctly identified (given names are highlighted in red and surnames appear in blue).
AQ2	Please provide country and date of patent application.
AQ3	Please verify the change in volume number in Ref. 3.
AQ4	Please check the figure 2, and provide the revised figure file if necessary.

Thank you for your assistance.

1 Ultrafast non-thermal laser excitation of gigahertz longitudinal and shear 2 acoustic waves in spin-crossover molecular crystals [$Fe(PM-AzA)_2(NCS)_2$]

3 T. Parpiiev,¹ M. Servol,² M. Lorenc,^{2,a)} I. Chaban,¹ R. Lefort,² E. Collet,² H. Cailleau,²
4 P. Ruello,¹ N. Daro,³ G. Chastanet,³ and T. Pezeril^{1,b)}

5 ¹Institut Molécules et Matériaux du Mans, UMR CNRS 6283, Université du Maine, 72085 Le Mans, France

6 ²Institut de Physique de Rennes, UMR CNRS 6251, Université de Rennes 1, 35042 Rennes, France

7 ³Institut de Chimie de la Matière Condensée de Bordeaux, UPR CNRS 9048, Université de Bordeaux,
8 33608 Pessac, France

9 (Received 17 July 2017; accepted 26 September 2017; published online xx xx xxxx)

10 We report GHz longitudinal as well as shear acoustic phonon photoexcitation and photodetection
11 using femtosecond laser pulses in a spin-crossover molecular crystal. From our experimental obser-
12 vation of time domain Brillouin scattering triggered by the photoexcitation of acoustic waves
13 across the low-spin (LS) to high-spin (HS) thermal crossover, we reveal a link between the molecu-
14 lar spin state and photoexcitation of coherent GHz acoustic phonons. In particular, we experimen-
15 tally evidence a non-thermal pathway for the laser excitation of GHz phonons. We also provide
16 experimental insights into the optical and mechanical parameters evolving across the LS/HS spin
17 crossover temperature range. *Published by AIP Publishing.* <https://doi.org/10.1063/1.4996538>

18 Understanding how ultrafast photoinduced molecular
19 switching in crystals couples to the lattice in optical materi-
20 als is one of the key challenges in the fields of ultrafast
21 photo-induced phase transitions or transformations and ultra-
22 fast acoustics. Systems like spin-crossover compounds
23 exhibit, with temperature or pressure, change of the molecu-
24 lar spin state in the central d^4 - d^7 transition metals of the
25 complex. They are promising candidates for diverse applica-
26 tions including miniature temperature sensors, displays, data
27 storage, and photonic devices.^{1,2} Moreover, they can be fab-
28 ricated in a variety of forms (bulk, powders, matrices, and
29 films) and down sizable to nanoparticles.² The possibility to
30 trigger their properties by light,³ especially in an ultrafast
31 fashion, offers further prospects in future applications as
32 optically controlled switching devices.^{2,4} While such com-
33 pounds have already been widely studied,⁵⁻⁸ there is a short-
34 age of information about the interplay between the change of
35 the molecular spin state, the change of the unit cell volume
36 (5% change), and the covalent bonding (10% change). From
37 this standpoint, the study of crystal deformations that trigger
38 excitation of coherent acoustic phonons clearly deserves fur-
39 ther experimental investigations. Until now,⁹ in the field of
40 photo-induced phase transitions or transformations in molec-
41 ular crystals, the role of coherent optical phonons has been
42 long under scrutiny because of the central role of optical
43 mode softening, whereas that of coherent acoustic phonons
44 and lattice deformations has not benefited from the same
45 surge of effort. It is of paramount importance from the
46 fundamental standpoint, as well as for the control of non-
47 volatile information and energy storage, to further explore
48 the pathways whereby acoustic phonons lead to non-volatile
49 photo-induced states.

50 In the following, we describe our experimental results
51 dealing with the photoexcitation of coherent acoustic phonons
52 in a spin-crossover crystal, performed at different temperatures

53 around the spin crossover temperature $T_{1/2}$. The possibility of
54 exciting with light pulse coherent acoustic phonons in a vari-
55 ety of materials is well known;^{10,11} however, unlike the longi-
56 tudinal acoustic phonons, the shear acoustic phonons are
57 difficult to photo-excite.^{12,13} Our results highlight peculiar and
58 efficient mechanisms for the photoexcitation of shear acoustic
59 phonons and shed light on the interplay between molecular
60 and elastic parameters in a spin-crossover compound.

61 In the present experiments sketched in Fig. 1(a),
62 spin-crossover molecular crystals [$Fe(PM-AzA)_2(NCS)_2$],
63 schematically represented in the inset of Fig. 1(b), were
64 investigated. These molecular crystals belong to the mono-
65 clinic space group $P2_1/c$ with one molecule as the asymmet-
66 ric unit. In agreement with Refs. 5 and 7, the smooth thermal
67 spin-crossover of these crystals with a spin crossover around
68 $T_{1/2} \sim 180$ K can be monitored experimentally from the mea-
69 surement of the magnetic susceptibility χ_M and the product
70 $\chi_M T$, as indicated in Fig. 1(b). The experiments were per-
71 formed on a parallelepipedic $4 \times 1 \times 1$ mm³ single crystal,
72 with smooth, black color surfaces.⁷ Due to large optical
73 absorption by the crystal, front side pump-probe transient
74 reflectivity measurements were performed, see Fig. 1(a). The
75 pump and probe beams originate from a femtosecond Ti-
76 Sapphire Coherent RegA 9000 regenerative amplifier operat-
77 ing at a central wavelength of 800 nm and delivering 160 fs
78 pulses at a repetition rate of 250 kHz. The 400 nm pump
79 pulses of about 40 nJ energy per pulse were focused on the
80 (110) surface of the crystal with a gaussian spatial profile of
81 FWHM ~ 100 μ m. The time delayed 800 nm probe of tenfold
82 weaker energy per pulse, vertically polarized, was tightly
83 focused at 30° oblique incidence on the (110) surface normal
84 to the crystal and spatially overlapped with the pump spot.
85 The reflected probe beam was directed to a photodiode cou-
86 pled to a lock-in amplifier operating at 50 kHz of the pump
87 laser modulation frequency, to measure transient differential
88 reflectivity $\Delta R(t)$ as a function of time delay between pump
89 and probe beams. Upon transient absorption of the 400 nm
90 pump pulse over the optical skin depth of the crystal, the light

a)Electronic mail: maciej.lorenc@univ-rennes1.fr

b)Electronic mail: thomas.pezeril@univ-lemans.fr

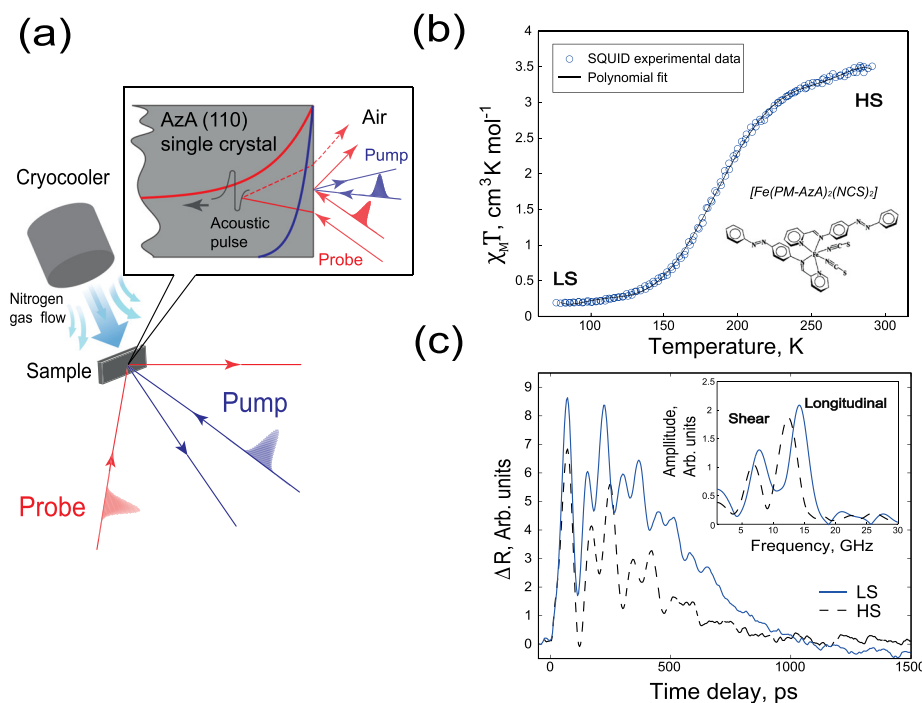


FIG. 1. (a) Sketch of the experimental setup. A laser pump pulse photoexcites the molecular crystal sample under continuous nitrogen flow for temperature control. The propagation of the photoexcited acoustic pulse is detected by a time-delayed optical probe pulse vertically polarized. (b) Schematic representation of the spin-crossover compound⁵ and its magnetic susceptibility recorded across the smooth thermal spin-crossover temperature $T_{1/2}$. (c) Transient reflectivity signals recorded in the LS and HS states. The frequency spectrum of the LS and HS Brillouin oscillations shown in the inset gathers crucial information on the photoexcitation of both longitudinal and shear acoustic phonons.

energy is partially converted into mechanical energy that drives the excitation of acoustic pulses propagating away from the free surface. In the present situation, the crystal is about five times less absorptive at 800 nm than at 400 nm, see Fig. S1 in the [supplementary material](#), such that it can be considered as semi-transparent at 800 nm and opaque at 400 nm. As a consequence, the pump light is locally absorbed at the free surface where it launches a propagating acoustic strain that backscatters the probe light from within the semi-transparent medium and leads to the occurrence of time domain Brillouin scattering oscillations, see Fig. 1(c). As in any Brillouin scattering process, the frequency ν of these oscillations is related to the ultrasound velocity v of the crystal, to the probe wavelength λ , to the refractive index n of the medium, and to the back-scattering angle θ through

$$\nu = 2 n v \cos \theta / \lambda. \quad (1)$$

The light activation of both longitudinal and shear acoustic polarizations, of different ultrasonic speeds v , leads to two distinct Brillouin frequencies. Figure 1(c) shows an example of such time domain Brillouin scattering light modulation where unambiguous periodic features at about 6 GHz and 12 GHz, see inset, are evidenced right after pump excitation at zero time delay. The shear acoustic nature of the 6 GHz frequency has been further experimentally confirmed from depolarized Brillouin scattering measurements, see Fig. S2 in the [supplementary material](#), which enhances the optical detection of shear acoustic waves.¹³

The experiments have been conducted at different temperatures ranging from 100 K, where almost 100% of molecules are in the low spin state, up to 300 K, where almost 100% of the molecules are in the high-spin state. Temperature steps of 10 K were performed with a continuous nitrogen flow. For each recorded time domain Brillouin scattering signal in the 100–300 K temperature range, we have numerically fitted the experimental data with a damped sinusoidal function

in the form $\sim A \exp(-t/\tau) \sin(2\pi\nu t + \phi)$, to retrieve the frequency ν , the damping time τ , the amplitude A , and the phase ϕ of each longitudinal and shear acoustic mode. Based on the results from ellipsometry available in the [supplementary material](#), which led to the observation of a slight variation of only a few percent of the optical refractive index of the crystal at different temperatures, the huge 15% change in Brillouin frequency in Fig. 2(a) is mainly due to a pronounced change in both longitudinal and shear acoustic speeds with temperature. According to Eq. (1) and the measured real part n_{\perp} of the index of refraction at the probe wavelength for vertically polarized light, see [supplementary material](#), we have computed the change in Brillouin frequency to extract the variation in longitudinal and shear acoustic speed with temperature. The results displayed in Fig. 2(b) confirm the substantial change in acoustic speed, in the range of 10%, further emphasizing the giant change in mechanical properties of the material across the spin crossover temperature. This intrinsic softening of the material at increasing temperature around $T_{1/2}$ is coupled to a substantial isostructural modification of the lattice parameters, manifested in the change of the unit cell volume by as much as $\sim 3\%$.^{5,14}

As a comparison with highly magnetostrictive ferromagnetic compounds such as Terfenol¹⁵ which is the foremost highest magnetostrictive alloy with a change of the unit cell volume by an amount of 0.1% upon modification of the magnetization vector, the change in $[\text{Fe}(\text{PM-AzA})_2(\text{NCS})_2]$ lattice parameters in the order of few % reveals the gigantic spin state-lattice coupling in these molecular materials. The pronounced molecular spin state-lattice coupling in such compounds is bound to influence the generation of coherent acoustic phonons.

The evolutions of the damping time coefficients with temperature displayed in Fig. 2(c) are linked to the imaginary part of the refractive index k_{\perp} at the probe wavelength and to the intrinsic acoustic attenuation. From the measured k_{\perp} at the probe wavelength, we have processed the measured

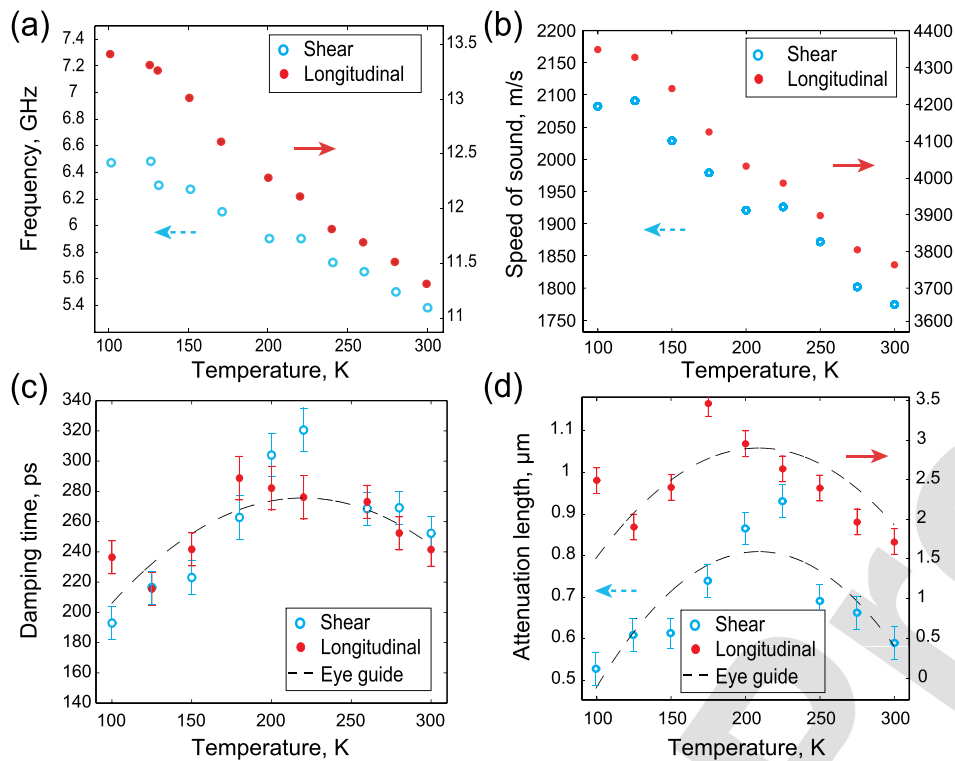


FIG. 2. From the time domain Brillouin scattering experimental data obtained for vertically polarized pump and probe beams at different temperatures, we have extracted the frequency (a) and the damping coefficient (c) of the measured Brillouin oscillations. In a second step, the temperature evolution of the index of refraction in the [supplementary material](#) led to the calculated acoustic speed (b) and acoustic attenuation length (d) of the longitudinal and shear acoustic modes across $T_{1/2}$. The eye guides are 2nd order polynomial fit of the extracted coefficients and the error bars are estimated from our experimental uncertainties.

AQ4

damping of the Brillouin oscillations τ , in order to extract the acoustic attenuation length Γ straightforwardly from $\Gamma = v\tau - \xi$, where v is the longitudinal or shear acoustic speed and $\xi = 4\pi k_{\perp}/\lambda$ is the optical penetration depth. Note that the deconvolution of the acoustic damping in the measured signals is not as straightforward in classical Brillouin spectroscopy which sometimes requires complicated analyses of the Brillouin linewidth of the peaks in the frequency domain.¹⁶ The result of the calculation of the acoustic attenuation length for both acoustic modes, longitudinal and shear, is displayed in Fig. 2(d). The remarkable maximum attenuation length measured in Fig. 2(d) highlights a decrease in the acoustic attenuation across the spin-phase crossover transition. In the present case, the phenomenon is reversed from the well-known structural α -relaxation which has been evidenced in glass forming liquids across the T_g glass transition temperature.¹⁷ The acoustic wave propagates on longer distances at the spin-crossover temperature which indicates that the structural modification of the lattice and the statistical growth or disappearance of the LS/HS states do not perturb the acoustic phonon propagation; on the contrary, the acoustic phonon propagation is facilitated during the spin crossover transition.

We can invoke several main mechanisms for the laser-driven lattice motion in the present spin-crossover material: the thermoelastic mechanism which is linked to the transient thermal dilation of the lattice following the temperature rise due to laser absorption and two non-thermal mechanisms, namely, the molecular spin state-lattice coupling mechanism¹⁸ and the deformation potential mechanism.¹³ The temperature evolution of the Brillouin amplitudes and Brillouin phases at two different pump polarizations [horizontal (H) and vertical (V) polarizations] displayed in Fig. 3 gathers crucial information on the photoacoustic excitation process. The fact that the optical index of refraction does not vary

significantly with temperature warrants that the measured Brillouin amplitude and phase are mainly sensitive to the excitation mechanisms and not to the detection process through a modification of the acousto-optic coefficients with temperature. Since the measurement of the Brillouin amplitude can suffer from experimental artifacts, such as beam pointing stability during sample heating or cooling, we have chosen to further process the longitudinal A_L and shear A_S Brillouin amplitudes data by taking the ratio of both amplitudes, defined as A_L/A_S , not biased by optical artifacts. This simple procedure highlights a discrepancy shown in Fig. 3(a) that cannot be assigned to the thermoelastic mechanism. In fact, as indicated by the difference in optical absorption coefficients k_{\perp} and k_{\parallel} at the pump wavelength, see [supplementary material](#), the laser induced temperature rise in such anisotropic crystals depends on the pump polarization. However, taking the ratio of amplitudes of both modes is a proper way to conveniently remove the temperature rise contribution in the thermoelastic process of acoustic excitation, similar for longitudinal and shear acoustic modes. Therefore, the gap between the amplitude ratio in Fig. 3(a) with H or V polarizations is assigned to a non-thermal mechanism, either molecular spin state-lattice coupling or deformation potential mechanism. One possible explanation of the observed amplitude jump would be the anisotropy in the deformation potential mechanism. The latter should be considered as tensorial in such crystals with different diagonal and non-diagonal coefficients referring to preferential electronic excitations of the ligands by horizontally or vertically polarized pump pulses, with some similarities with Ref. 19 that demonstrates the wide range of electronic excitations of organic molecules that can drive coherent lattice phonon excitation. In addition to the electron deformation potential mechanism, we cannot neglect the molecular spin state-lattice coupling anisotropy, thus revealing pump laser polarization dependence.

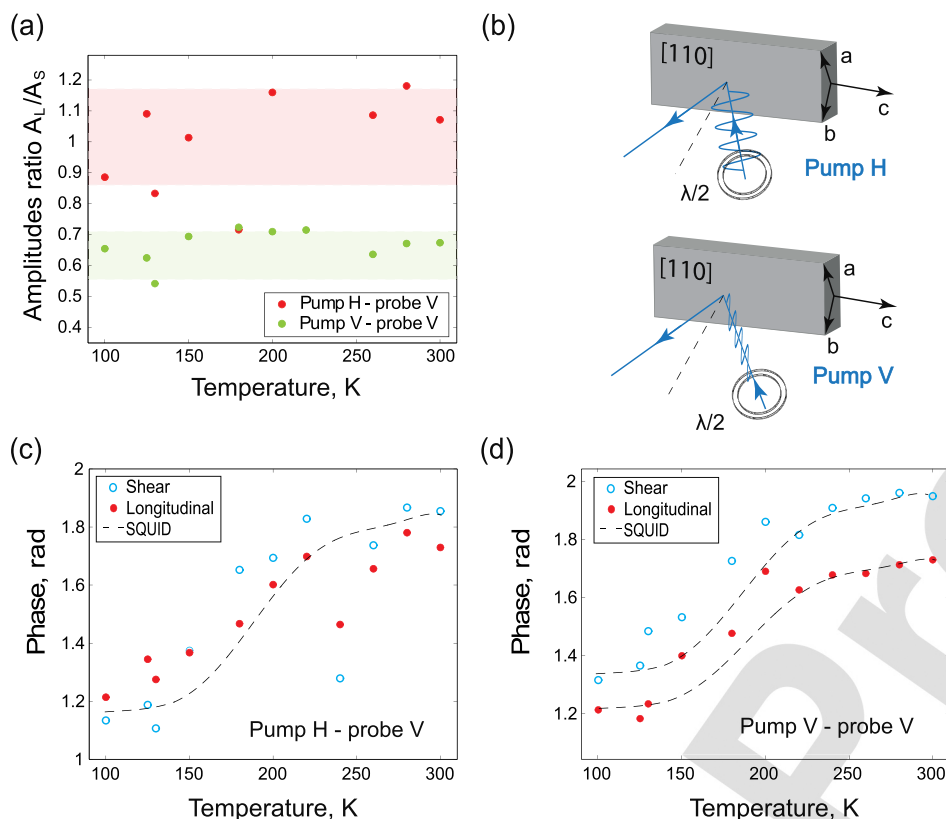


FIG. 3. (a) Ratio between the longitudinal and shear Brillouin amplitudes for different pump polarizations. Red dots correspond to the horizontally polarized pump and green to the vertically polarized pump, as sketched in (b). Extracted time domain Brillouin phase for horizontally (c) and vertically (d) polarized pump beams of both longitudinal and shear acoustic modes in the compound at different crystal temperatures. The SQUID curve matches the Brillouin phase evolution across $T_{1/2}$.

Another striking feature suggesting coexistence of photoacoustic mechanisms is revealed by the Brillouin phase change in Figs. 3(c) and 3(d) with H or V pump polarizations. Once again, if we assume that the slight change with temperature of the optical index of refraction is irrelevant for the interpretation of our experimental observations, the substantial phase jump in the range of 0.6 radians of both longitudinal and shear Brillouin signals across the spin-crossover transition highlights a profound change in the laser-matter mechanism for acoustic phonons excitation. Based on Ref. 20, we can interpret this phase change, which correlates with the magnetic susceptibility of Fig. 1(b), as a change in the acoustic excitation process through the contribution of the spin state-lattice mechanism that vanishes once the compound reaches 100% HS spin. However, the photoinduced spin state-lattice coupling is maybe not the most efficient at this pump wavelength. Therefore, we cannot rule out the deformation potential mechanism as relevant in the process of laser excitation of coherent acoustic phonons in the present spin crossover material. The observation of the phase jump of about 0.2 radians in Fig. 3(d) between longitudinal and shear excitation points to a non-thermal mechanism of acoustic excitation sensitive to the pump polarization, as in Fig. 3(a). As a matter of fact, based on the results presented in Fig. 3, we can conclude that two non-thermal mechanisms are triggered in these molecular crystals, each one having different efficiency (amplitudes) and characteristic times (phases).

In summary, we have performed ultrafast time-domain Brillouin scattering experiments to study non equilibrium dynamics following femtosecond photoexcitation of spin-crossover molecular crystals $[Fe(PM-AzA)_2(NCS)_2]$. We have presented results for coherent GHz acoustic phonons photogeneration and photodetection in a spin-crossover material

across the spin-crossover temperature range. Through time domain Brillouin scattering, we evidence non-thermal excitation of acoustic phonons which are of spin state-lattice coupling and/or deformation potential origin. Experimentally revealed on the sub-nanosecond time-scale, remarkable sensitivity of Brillouin frequencies to the spin state of a molecular material opens advanced perspectives for probing macroscopically relevant processes during a phase transition. We envisage pump-pump-probe experiments, in which the molecular spin-state is photoexcited with wavelength tuned pump pulse, while the real-time coupling of thus generated spin-states to the lattice is followed by the second pump through time-resolved Brillouin scattering, such as this work. Furthermore, our results highlight the versatile and efficient generation of ultrashort shear acoustic phonons for future investigations of viscoelastic properties of materials such as liquids,²¹ glasses,^{22,23} mixed multiferroics, correlated electron systems, and magnetic materials. Ultimately, deeper knowledge of the spin state-elastic coupling in spin-crossover molecular crystals will be crucial for the design of multifunctional molecular devices.

See supplementary material for the temperature data of the real n and imaginary k refractive index of $[Fe(PM-AzA)_2(NCS)_2]$ at 400 nm and 800 nm wavelengths, as for a comparison between transient reflectivity and depolarized Brillouin scattering.

The authors are thankful to Pr. Vitalyi Gusev for beneficial scientific discussions and guidance and to Lionel Guilmeau for technical support. The authors gratefully acknowledge Agence Nationale de la Recherche for financial support under grants ANR-16-CE30-0018, ANR-14-CE26-0008, and ANR-12-BS09-0031-01.

- ¹J.-F. Létard, P. Guionneau, and L. Goux-Capes, *Top. Curr. Chem.* **235**, 221 (2004). 321
- ²A. Bousseksou, G. Molnár, L. Salmona, and W. Nicolazzia, *Chem. Soc. Rev.* **40**, 3313 (2011). 322
- ³A. Hauser, J. Jeftić, H. Romstedt, R. Hinek, and H. Spiering, *Coord. Chem. Rev.* **190–192**, 471 (1999). 323
- ⁴J.-F. Létard and E. Freysz, patent WO2012010801 A1 (■ ■ 2012). 324
- ⁵P. Guionneau, J.-F. Létard, D. S. Yufit, D. Chasseau, G. Bravic, A. E. Goeta, J. A. K. Howard, and O. Kahn, *J. Mater. Chem.* **9**, 985–994 (1999). 325
- ⁶A. Goujon, F. Varret, K. Boukheddaden, C. Chong, J. Jeftić, Y. Garcia, A. D. Naik, J. C. Ameline, and E. Collet, *Inorg. Chim. Acta* **361**, 4055 (2008). 326
- ⁷A. Marino, M. Servol, R. Bertoni, M. Lorenc, C. Mauriac, J.-F. Létard, and E. Collet, *Polyhedron* **66**, 123 (2013). 327
- ⁸Y. Jiang, L. Chung Liu, H. M. Muller-Werkmeister, C. Lu, D. Zhang, R. L. Field, A. Sarracini, G. Moriena, E. Collet, and R. J. Dwayne Miller, *Angew. Chem. Int. Ed.* **56**, 7130 (2017). 328
- ⁹R. Bertoni, M. Lorenc, H. Cailleau, A. Tissot, J. Laisney, M.-L. Boillot, L. Stoleriu, A. Stancu, C. Enachescu, and E. Collet, *Nat. Mater.* **15**, 606 (2016). 329
- ¹⁰J.-F. Létard, J. A. Real, N. Moline, A. B. Gaspar, L. Capes, O. Cador, and O. Kahn, *J. Am. Chem. Soc.* **121**, 10630–10631 (1999). 330
- ¹¹C. Thomsen, H. T. Grahn, H. J. Maris, and J. Tauc, *Phys. Rev. B* **34**, 4129 (1986). 331
- ¹²T. Pezeril, P. Ruello, S. Gougeon, N. Chigarev, D. Mounier, J.-M. Breteau, P. Picart, and V. Gusev, *Phys. Rev. B* **75**, 174307 (2007). 332
- ¹³T. Pezeril, *J. Opt. Laser Technol.* **83**, 177 (2016). 333
- ¹⁴N. Klinduhov, D. Chernyshov, and K. Boukheddaden, *Phys. Rev. B* **81**, 094408 (2010). 334
- ¹⁵O. Kovalenko, T. Pezeril, and V. Temnov, *Phys. Rev. Lett.* **110**, 266602 (2013). 335
- ¹⁶J. R. Sandercock, *Light Scattering in Solids III* (Springer Berlin Heidelberg, Berlin, 1982), pp. 173–206. 336
- ¹⁷Y. Yang and K. A. Nelson, *J. Chem. Phys.* **103**, 7732 (1995). 337
- ¹⁸C. Enachescu, L. Stoleriu, M. Nishino, S. Miyashita, A. Stancu, M. Lorenc, R. Bertoni, H. Cailleau, and E. Collet, *Phys. Rev. B* **95**, 224107 (2017). 338
- ¹⁹A. Rury, S. Sorenson, and J. Dawlaty, *J. Chem. Phys.* **144**, 104701 (2016). 339
- ²⁰G. Vaudel, T. Pezeril, A. Lomonosov, M. Lejman, P. Ruello, and V. E. Gusev, *Phys. Rev. B* **90**, 014302 (2014). 340
- ²¹T. Pezeril, C. Klieber, S. Andrieu, and K. A. Nelson, *Phys. Rev. Lett.* **102**, 107402 (2009). 341
- ²²C. Klieber, T. Pezeril, S. Andrieu, and K. A. Nelson, *J. Appl. Phys.* **112**, 013502 (2012). 342
- ²³C. Klieber, T. Hecksher, T. Pezeril, D. Torchinsky, J. Dyre, and K. Nelson, *J. Chem. Phys.* **138**, 12A544 (2013). 343